White Rose Research Online

eprints@whiterose.ac.uk
https://eprints.whiterose.ac.uk
Universities of Leeds, Sheffield and York

Deposited via The University of Sheffield.

White Rose Research Online URL for this paper:
https://eprints.whiterose.ac.uk/id/eprint/125962/

Version: Accepted Version

Article:
Bezzina, J.P., Prendergast, M.B., Blanksby, S.J. et al. (2018) Gas-phase oxidation of the protonated uracil-5-Yl radical cation. Journal of Physical Chemistry A, 122 (4). pp. 890-896. ISSN: 1089-5639

https://doi.org/10.1021/acs.jpca.7b09411

This document is the Accepted Manuscript version of a Published Work that appeared in final form in Journal of Physical Chemistry A, copyright © American Chemical Society after peer review and technical editing by the publisher. To access the final edited and published work see https://doi.org/10.1021/acs.jpca.7b09411

Reuse
Items deposited in White Rose Research Online are protected by copyright, with all rights reserved unless indicated otherwise. They may be downloaded and/or printed for private study, or other acts as permitted by national copyright laws. The publisher or other rights holders may allow further reproduction and re-use of the full text version. This is indicated by the licence information on the White Rose Research Online record for the item.

Takedown
If you consider content in White Rose Research Online to be in breach of UK law, please notify us by emailing eprints@whiterose.ac.uk including the URL of the record and the reason for the withdrawal request.

UNIVERSITY OF LEEDS
University of Sheffield
UNIVERSITY of York

THE JOURNAL OF PHYSICAL CHEMISTRY A

Subscriber access provided by The University Library | University of Sheffield

Article

Gas-Phase Oxidation of the Protonated Uracil-5-Yl Radical Cation

James P. Bezzina, Matthew B. Prendergast, Stephen J. Blanksby, and Adam J Trevitt

J. Phys. Chem. A, **Just Accepted Manuscript** • DOI: 10.1021/acs.jpca.7b09411 • Publication Date (Web): 03 Jan 2018

Downloaded from http://pubs.acs.org on January 8, 2018

Just Accepted

"Just Accepted" manuscripts have been peer-reviewed and accepted for publication. They are posted online prior to technical editing, formatting for publication and author proofing. The American Chemical Society provides "Just Accepted" as a free service to the research community to expedite the dissemination of scientific material as soon as possible after acceptance. "Just Accepted" manuscripts appear in full in PDF format accompanied by an HTML abstract. "Just Accepted" manuscripts have been fully peer reviewed, but should not be considered the official version of record. They are accessible to all readers and citable by the Digital Object Identifier (DOI®). "Just Accepted" is an optional service offered to authors. Therefore, the "Just Accepted" Web site may not include all articles that will be published in the journal. After a manuscript is technically edited and formatted, it will be removed from the "Just Accepted" Web site and published as an ASAP article. Note that technical editing may introduce minor changes to the manuscript text and/or graphics which could affect content, and all legal disclaimers and ethical guidelines that apply to the journal pertain. ACS cannot be held responsible for errors or consequences arising from the use of information contained in these "Just Accepted" manuscripts.

ACS Publications

The Journal of Physical Chemistry A is published by the American Chemical Society. 1155 Sixteenth Street N.W., Washington, DC 20036

Published by American Chemical Society. Copyright © American Chemical Society. However, no copyright claim is made to original U.S. Government works, or works produced by employees of any Commonwealth realm Crown government in the course of their duties.

Gas-phase Oxidation of the Protonated Uracil-5-yl Radical Cation

James P. Bezzina,[†] Matthew B. Prendergast,[†] Stephen J. Blanksby,[‡] and Adam J. Trevitt[*,†]

[†]*School of Chemistry, University of Wollongong, Wollongong, Australia, 2522*

[‡]*Central Analytical Research Facility, Institute for Future Environments, Queensland University of Technology, Brisbane, Australia 4001*

E-mail: adamt@uow.edu.au

Phone: +61 2 4221 5545

Abstract

This study targets the kinetics and product detection of the gas-phase oxidation reaction of protonated 5-dehydrouracil (uracil-5-yl) distonic radical cation using ion-trap mass spectrometry. Protonated 5-dehydrouracil radical ion (5-dehydrouracilH$^+$ radical ion, m/z 112) is produced within an ion trap by laser photolysis of protonated 5-iodouracil. Storage of the 5-dehydrouracilH$^+$ radical ion in the presence of controlled concentration of O_2 reveals two main products. The major reaction product pathway is assigned as the formation of protonated 2-hydroxypyrimidine-4,5-dione (m/z 127) + OH. A second product ion (m/z 99), putatively assigned as a 5-member-ring ketone structure, is tentatively explained as arising from the decarbonylation (– CO) of protonated 2-hydroxypyrimidine-4,5-dione. Because protonation of the 5-dehydrouracil radical likely forms a di-enol structure, the O_2 reaction at the 5 position is *ortho* to an –OH group. Following this addition of O_2, the peroxyl radical intermediate isomerises by H atom transfer from the –OH group. The ensuing hydroperoxide then decomposes to eliminate OH radical. It is shown that this elimination of OH radical (–17 Da) is evidence for the presence of an –OH group *ortho* to the initial phenyl-radical site, in good accord with calculations. The subsequent CO loss mechanism, to form the aforementioned 5-member-ring structure, is unclear but some pathways are discussed. By following the kinetics of the reaction, the room temperature second order rate coefficient of the 5-dehydrouracilH$^+$ distonic radical cation with molecular oxygen is measured at 7.2×10^{-11} cm^3 molecule^{-1} s^{-1}, $\Phi = 12\%$ (with $\pm 50\%$ total accuracy). For aryl radical reactions with O_2, the presence of OH elimination product pathway, following the peroxyl radical formation, is a indicator of an –OH group *o*rtho to the radical site.

Introduction

In DNA, bromouracil and iodouracil can be substituted for thymine units without major disruption to DNA structure. Subsequent homolytic dehalogenation – either by electron bombardment or photolysis – leads to the formation of uracil-5-yl radicals and can initiate DNA-strand breaking[1] and DNA-protein cross-linking.[2] As such, iodo and bromouracil photolytic strategies have been extensively investigated for targeted cancer therapies. This photochemistry can also be used to probe DNA structure.[3,4] To elucidate the underlying mechanisms, studies have examined the reactivity of these uracil-5-yl σ-radicals within nucleosides and DNA strands.[4–6] Recently, further insights have been reported on the photophysics of 5-iodouracil[7] as well as the negative-ion states (made from electron attachment) of 5-bromo and 5-iodouracil thought to be involved in the dissociative electron capture mechanism.[8]

A key process, that ultimately results in DNA strand-cleavage, involves uracil-5-yl radicals abstracting H atoms from nearby functional groups.[9,10] Alternatively, several studies have investigated the possibility that, under aerobic conditions, reaction of the uracil-5-yl radicals with molecular oxygen will form peroxyl radical intermediates (Scheme 1 (i)), and that these peroxyl radicals might be key intermediates in rationalising the activity of these halouracils.[11,12] Following this line of enquiry, Schyman *et al.* reported in a computational study that the peroxyl radical would actually be a less efficient at H atom abstraction from deoxyribose than the uracil-5-yl parent.[13] However, following our recent work on ortho-hydroxylphenyl radicals, which showed characteristic reaction pathways,[14] we posit that the enol form of the uracil-5-yl radical, with an OH group adjacent to the radical at the 5 position, will significantly change the outcome the radical reaction with O_2. Thus we set out to investigate the gas-phase reaction of protonated uracil-5-yl radical cation, which should be in the enolic form. In has also been shown that studies on protonated uracils and uridines provide important insight into the stability and prevalence of various tautomeric forms.[15–17] Combining ion trap mass spectrometry and the investigation of charge-separation distonic

radical ions is a insightful technique for the study of radical reactivity without the perturbative presence of solvent.[18–20]

In this paper, we explore the O_2 reaction with protonated uracil-5-yl (5-dehydrouracilH$^+$ radical). We show that the radical of the protonated di-enol form shown in Scheme 1 (ii) has access to a unique and efficient reaction pathways afforded by the presence of the it ortho –OH group. This leads to the production of a di-one species with elimination of OH radical. It also appears that in the gas-phase, the quinone might spontaneously decarbonylate in considerable yield. Both the elimination of OH and the detection of a subsequent decarbonylation product are characteristic signatures of beta-hydroxy peroxy radicals in aromatic systems.

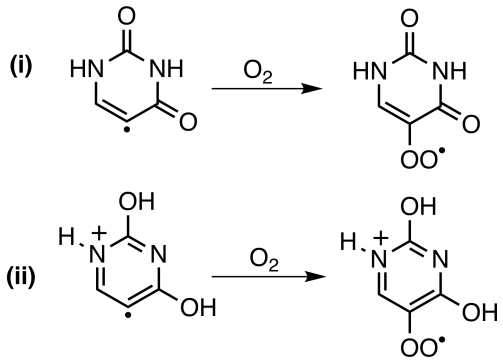

Scheme 1: Molecular oxygen addition to (i) 5-dehydrouracil radical and (ii) protonated 5-dehydrouracil radical ion

Experimental Methods

Experiments were performed on a Thermo Fisher Scientific LTQ-XL linear quadrupole ion-trap mass spectrometry, which was modified to allow the passage of laser photons through the ion trap. Modifications to the buffer-gas delivery manifold allowed for the controlled introduction of gas-phase reactants, in this case O_2. Protonated ions were introduced into the mass spectrometer by injecting methanol solutions containing 5-15 µM 5-iodouracil (Sigma-Aldrich) via an electrospray ion (ESI) source operated in positive ion mode. The pressure

within the ion trap is approximately 2.5 mTorr and the effective ion temperature within these linear quadrupole ion traps has been recently estimated at 318 ± 23 K,[21] consistent with an earlier estimate of 307 K.[22]

For the photolytic preparation of protonated radical ions from suitable precursors, the ion-trap mass spectrometer has been modified by installation of a vacuum compatible quartz window to the backing plate of the vacuum chamber.[23] This allows for laser access down the principle axis of the linear ion trap. Fixed wavelength photodissociation experiments were conducted using an unfocused Minilite Nd:YAG laser operating at 266 nm (∼1 mJ/pulse). This laser produces ∼5 ns pulses that were synchronised by the activation-synced trigger output from the mass spectrometer such that only a single laser pulse irradiates the target ion population per MS cycle.

To probe the reaction of radical ions with O_2, the helium buffer gas supplied to the ion trap was doped with 770±45 ppm O_2. The oxygen concentration within the trap was measured each day using a known calibration reaction (4-(*N,N,N*-trimethylammonium)phenyl radical cation + O_2 as reported by Kirk *et al.*[19]). All mass spectra shown here are an average of 50 scans. Kinetic traces are constructed from mass spectra acquired after varying ion storage times with each point in a kinetic trace representing an average ion abundance over 25 individual scans. Full pseudo-first order rate coefficient measurements were repeated on five different days.

The radical precursor 5-iodouracil (98%) was purchased from Sigma Aldrich, HPLC grade methanol and formic acid were purchased from Ajax Fine Chemicals (Sydney, Australia) and 770±45 ppm oxygen doped helium gas cylinder was purchased from BOC gases (Sydney, Australia). All commercial compounds were used without additional purification.

Quantum chemical calculations were performed using Gaussian 09.[24] Ground state energies of the 5-dehydrouracil radical protonation isomers were calculated using G4MP2-6x theory[25] with 6-311+G(2df,p) basis set. The remaining calculations were performed using the G3X-K composite method as described in Reference 26. XYZ coordinate tables for stationary points presented in the potential energy diagrams are included in the Supporting Information.

Results and Discussion

Ion-trap mass spectrometry

Figure 1 (a) shows a mass spectrum acquired following isolation and subsequent photodissociation of 5-iodouracilH$^+$ (5IURA, m/z 239) at λ = 266 nm ($PD_{266\,nm}$). The peak at m/z 112 is assigned as 5-dehydrouracilH$^+$ radical (5DHU, m/z 112) resulting from C–I bond homolysis as outlined in Scheme 2, where the protonation isomer (protomer) is assumed to be the most stable protomer, as described in more detail below. For comparison with conventional collision-induced dissociation (CID), subjecting m/z 239 to CID yields multiple dissociation products (Supplementary Figure S1) including minor amounts of m/z 112 and major product ions at m/z 222, 221 and 196. These major product ions are analogous to product channels observed in CID studies of protonated uracil.[27–30] Isolation of m/z 112 generated from CID and subsequent storage in the presence of O_2 shows similar products to the PD generated m/z 112 however a significant portion of m/z 112 remained unreacted (Supplementary Figure S2). This suggests that CID induces significant amounts of isomerisation in the radical population). This is consistent with previous studies by Kenttamaa and coworkers where laser synthesis of distonic radical ions were shown to produced greater yields of un-isomerised radicals compared with collision-activation methods.[31] As the focus of the current study is the reactivity of the 5DHU radical cation (m/z 112) no further study of the CID activated m/z 239 ion was pursued, and all m/z 112 ions herein are formed from $PD_{266\,nm}$.

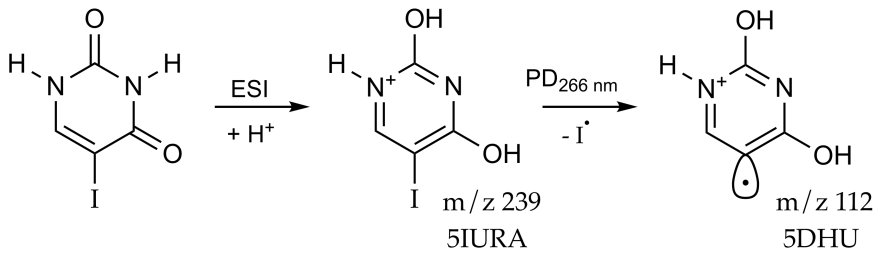

Scheme 2: General scheme for making the protonated 5-dehydrouracil radical ion in an ion-trap mass spectrometer.

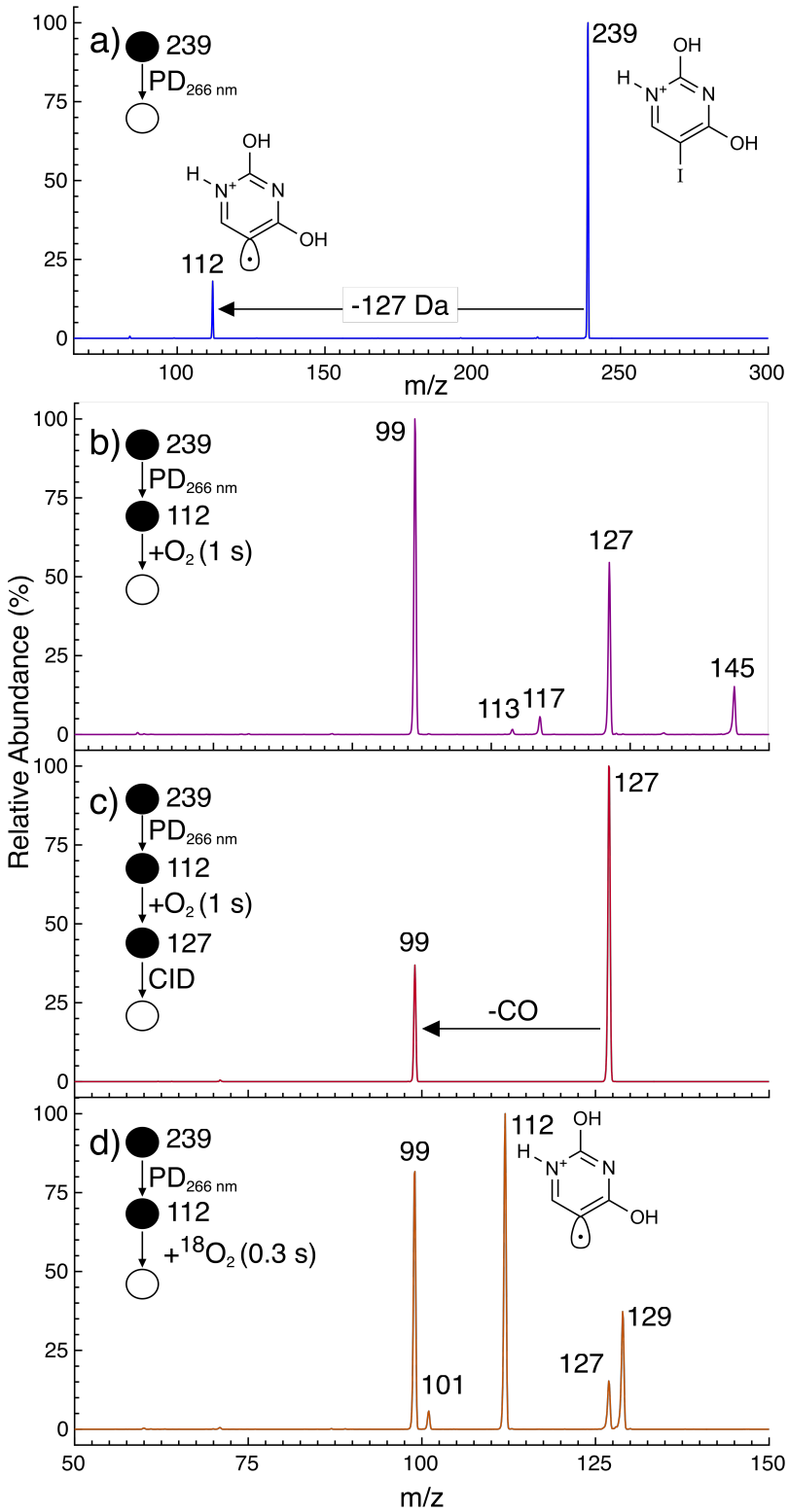

Figure 1: (a) Photodissociation mass spectrum (λ=266 nm) of isolated 5IURA cation, m/z 239, forming m/z 112. (b) Mass spectrum acquired after 1 s trap storage of 5DHU in the presence of O_2. (c) CID mass spectrum of isolated m/z 127 product species. (d) Mass spectrum of isolated 5DHU and reaction with $^{18}O_2$ (the small amount of m/z 127 is due to background $^{16}O_2$ present within the ion trap).

It has been reported that the most stable gas-phase protonation isomer (protomer) of uracilH$^+$ is protonation at the N1 position corresponding to a di-enol form.[32–35] Our G4MP2-6x calculations show that the thermodynamically preferred gas-phase protonation site of the 5-dehydrouracilH$^+$ radical is probably the analogous species (as shown in Scheme 2), however other protonation sites are within 7 kcal/mol (Table S1) so considering the closeness of these energies, and the fact that the ordering of relative protomer energies can be method dependent,[36] the presence of other protonation isomers cannot be ruled out.

The m/z 112 product ion (M) from $PD_{266\,nm}$ of 5IURA was isolated and stored within the ion trap in the presence of a controlled O_2 concentration with varying storage times. Figure 1 (b) is the product mass spectrum resulting from isolation of m/z 112 and storage for 1000 ms and it reveals that the m/z 112 ion has almost completely reacted, with the main product ions recorded at m/z 99, 117, 127 and 145. It is notable that these product ions do not correspond to either O_2 [M + 32] or O atom addition [M + 16], which are characteristic to distonic phenyl radical cation reactions with molecular oxygen.[19] The product ion at m/z 127 [M + 15] is consistent with O_2 addition (+32 Da) and subsequent OH loss (-17 Da), via a peroxyl-radical intermediate (M + 32), and is assigned as protonated 2-hydroxypyrimidine-4,5-dione, referred to as UBQ (uracil benzoquinone) henceforth, as depicted in Scheme 3 Ia. The peroxyl adduct (m/z 144) cation is not detected in these experiments, presumably due to its short lifetime. The m/z 99 product, corresponding to [M − 13], is assigned as arising from consecutive losses of OH (17 Da) and CO (28 Da) from the peroxyl radical intermediate, as investigated further below. Figure 1(c) shows that the CID activation of isolated m/z 127 leads to the exclusive formation of m/z 99 that we attribute to the loss of CO (decarbonylation) from m/z 127. This link between m/z 127 and 99 will be revisited in more detail below.

To confirm the assignment of m/z 127 and 99 as O_2 reaction products, the reaction of 5DHU was repeated with isotopically labelled $^{18}O_2$ gas and a product spectrum, after 300 ms

trapping time, is shown in Figure 1 (d). Comparing to Figure 1 (b), the detection of a new product at m/z 129 is consistent with $^{18}O_2$ and subsequent ^{18}OH loss, with a small amount of m/z 127 due to background $^{16}O_2$ present within the ion trap. The m/z 99 signal is consistent with C^{18}O loss (30 Da) from m/z 129 as shown in Scheme 4 as pathway (i), which dominates over the C^{16}O loss product ion at m/z 101 (28 Da) (pathway (ii)). This strong preference toward (i) over (ii) may assist in rationalising the decarbonylation mechanism which is discussed further below. Other ions observed at m/z 117 and 145 in Figure 1(b) are assigned as the addition of background water (+18 Da) to the reaction product ions at m/z 99 and 127, respectively. The small ion signal at m/z 113 in Figure 1(b) is possibly a H-atom addition product to m/z 112, perhaps from abstraction from background methanol (the ESI solvent) but it not considered in further detail here.

Kinetic measurements

Figure 2 contains representative kinetic traces, from one experiment, for the major species detected for the isolation and storage of m/z 112 ions in the presence of O_2 for storage times between (a) 0–350 ms and (b) 0–3000 ms. These data were acquired under the same experimental conditions as in Figure 1 (b) and are well described by a single exponential function in the case of m/z 112, 117 and 145. Fitting a sum of both an exponential growth and decay function was required for product ions m/z 99 and 127.

Table 1: Pseudo first-order rates for the species involved in the reaction of 5DHU with O_2 in the gas phase, with uncertainties reported as two standard deviations (2σ) obtained from the fits.

m/z	Decay k' (s^{-1})	Growth k' (s^{-1})
112	18.7 ± 0.1	-
127	0.5 ± 1.0	17 ± 6
99	0.2 ± 1.2	18 ± 4
117	-	0.1 ± 0.4

145	-	0.5 ± 0.4

Table 1 lists the fitted pseudo-first order rates extracted from fits in Figure 2(b). The *m/z* 112 (5DHU) ion decays away within 300 ms with *k*' = 18.7±0.1 s^{-1} and a small non-zero baseline of less than a 1% of the starting intensity indicates the presence of a very small fraction of isomerised, non-reactive *m/z* 112 radical ions. The product ions, *m/z* 127 and 99, grow in with matched *k*' values at 17±6 s^{-1} and 18±4 s^{-1}. Figure 2(b) shows that after formation, *m/z* 127 and 99 undergo subsequent reaction.

The *k*' values for decay of *m/z* 127 and 99 (*k*' = 0.5±1.0 s^{-1} and 0.2±1.2 s^{-1}) are reasonable well-matched to the growth of two slow forming species at *m/z* 145 and 117 (*k*' = 0.5±0.4 s^{-1} and 0.1±0.4 s^{-1}, respectively). The large uncertainty values associated with these low *k*' values is a result of the longer lifetimes not being fully captured by the time window of the experiment. These measurements were repeated over 12 experiments of the form presented in Figure 2, across 5 different days. Table 2 lists the [O_2] values determined for each day, the *k*' values for 5DHU (*m/z* 112) and corresponding second-order rate coefficients (k_{2nd}). Second-order rate coefficients (k_{2nd}, cm^3 $molecule^{-1}$ s^{-1}) and reaction efficiencies (ϕ) derived from fitted pseudo-first order rate coefficients (*k*') are reported in Table 3. Collision frequencies were calculated using a simple Langevin collision model.[37] Due mostly to the uncertainty in determining the absolute pressure within the ion trap, in addition to the accumulation of other experimental uncertainties, we ascribe an absolute experimental accuracy of ±50% to these experimental second-order rate coefficients.

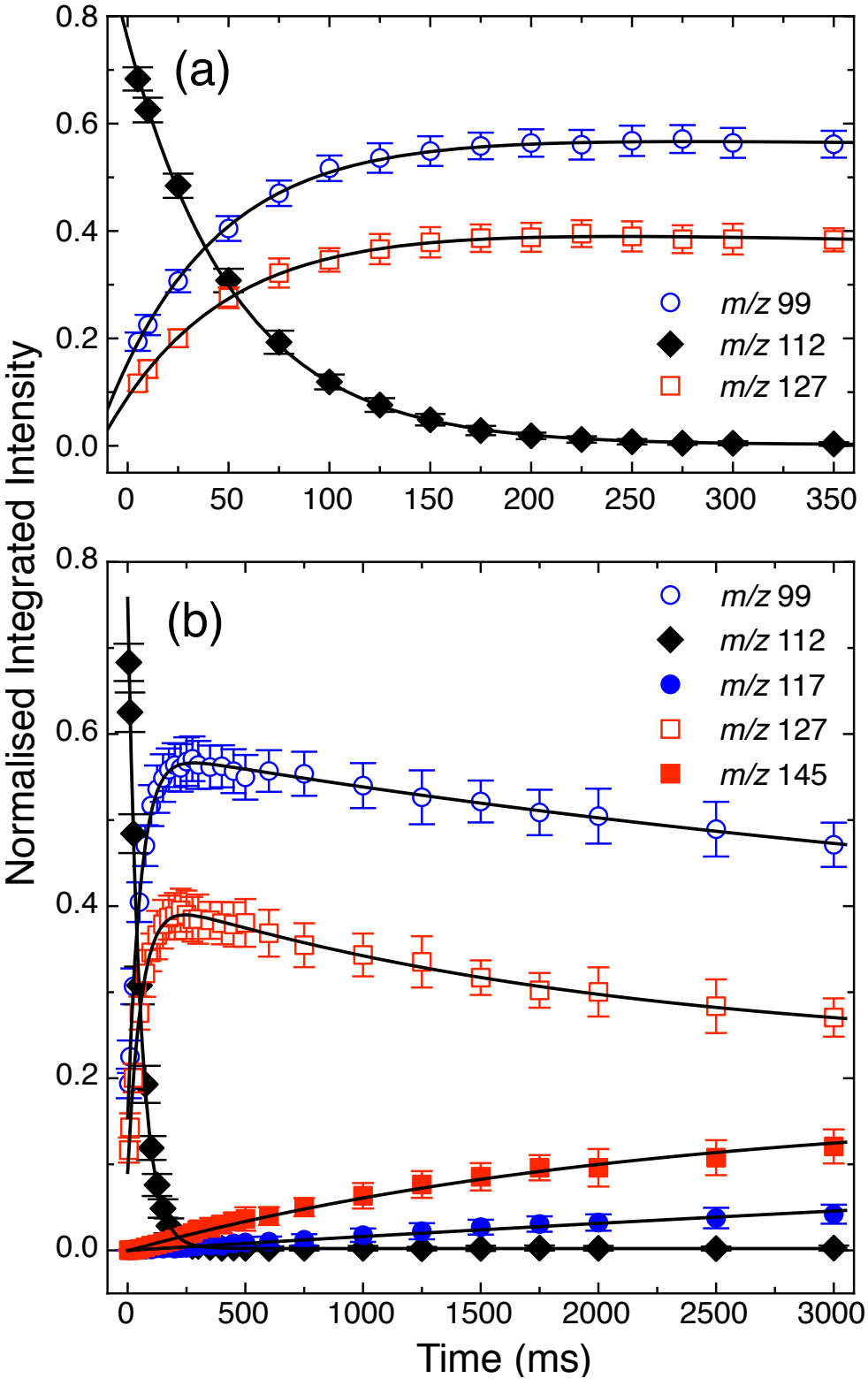

Figure 2: Kinetic profile of each major ion of the reaction of m/z 112 with O_2 spanning (a) $0-350$ ms and (b) $0-3000$ ms. Plotted are the product ions at m/z 99, 117, 127 and 145 fitted with an exponential function or a combined growth and decay exponential function (black line) as described in the text. Error bars are $\pm 2\sigma$.

Table 2: Comparison of the oxygen concentration, the pseudo-first order rate coefficients and second-order rate coefficients of m/z 112 derived for each experimental run. Uncertainties reported as 2σ representing experimental precision.

Experimental Day	$[O_2]$ (molecule cm^{-3})	k' (s^{-1})	k_{2nd} (cm^3 molecule^{-1} s^{-1})
1	$2.9 \pm 0.5 \times 10^{11}$	19.4 ± 0.8	$6.6 \pm 0.9 \times 10^{-11}$
2	$2.7 \pm 0.5 \times 10^{11}$	20.6 ± 0.6	$7.5 \pm 0.9 \times 10^{-11}$
3	$2.9 \pm 0.6 \times 10^{11}$	20.7 ± 0.6	$7.2 \pm 0.9 \times 10^{-11}$
4	$2.7 \pm 0.7 \times 10^{11}$	21.0 ± 1.0	$8.0 \pm 2.0 \times 10^{-11}$
5	$2.9 \pm 0.6 \times 10^{11}$	18.9 ± 0.9	$7.0 \pm 1.0 \times 10^{-11}$
Average			$7.2 \pm 0.6 \times 10^{-11}$

Table 3: The average second-order rate coefficients for 5DHU ($\pm 2\sigma$) compared with literature values for other reaction of O_2 with distonic phenyl radical cations.

Distonic Radical Cation	k_{2nd} (cm^3 molecule^{-1} s^{-1})	Φ (%)	Reference
5-DehydrouracilH$^+$ radical	$7.2 \pm 1.1 \times 10^{-11}$	12	This study
4-(*N,N,N*-Trimethyl-ammonium)-phenyl radical	2.8×10^{-11}	5	Kirk *et al.*[19]
5-(*N,N,N*-Trimethyl-ammonium)-2-hydroxyphenyl	2.5×10^{-11}	4	Prendergast *et al.*[14]
5-(*N,N,N*-Trimethyl-ammonium)-2-methylphenyl	2.9×10^{-11}	5	Prendergast *et al.*[38]

The average second-order rate constant (k_{2nd}) for this reaction is 7.2×10^{-11} cm^3 molecule^{-1} s^{-1} with a reaction efficiency of 12%, which is significantly greater than the k_{2nd} and reaction efficiency values reported for other distonic aryl radical cations.[19,38] The 12% efficiency is close to the 15% reported for distonic anion 2-carboxylatophenyl + O_2 which is one of the

largest O_2 reaction efficiencies for an aromatic distonic ions + O_2 reaction reported in Kirk *et al.*[19] where 11 distonic phenyl-type radicals are compared and have reaction efficiency that spans 5-15%. The neutral phenyl + O_2 reaction efficiency is around 4-5% (see Kirk *et al.*[19] and references therein).

Reaction mechanism and products

It is known that tyrosyl radicals,[39] *ortho*-substituted methylphenyl[38,40] and hydroxyphenyl radicals[14] react with O_2 and subsequently eliminate $^{\bullet}$OH via a mechanism analogous to the Waddington mechanism for the β-hydroxyl radical oxidation of alcohols[41] and it is apparent that the same pattern is observed here. A calculated potential energy diagram for an OH elimination mechanism is shown in Figure 3. The O_2 addition adduct reaction is -42 kcal mol^{-1} exothermic and the H atom transfer from the –OH group, *ortho* to the peroxy radical, to form the hydroperoxide is then about 10 kcal mol^{-1} uphill. Attempts to locate a transition state between those two intermediates were unsuccessful. The elimination of OH can then occur through a transition state at -14.7 kcal mol^{-1} below the entrance channel. The UBQ + $^{\bullet}$OH reaction enthalpy is calculated at -20.9 kcal mol^{-1}.

The strong signal at *m/z* 99 in Figure 1 (b) requires more thought. Our conclusion is that either the *m/z* 99 ion is formed from the prompt decarbonylation of nascent UBQ (*m/z* 127) product or that there is a 3-body elimination channel from the O_2 adduct surface. The matched growth rates of *m/z* 127 and *m/z* 99 do not unambiguously differentiate between these two possibilities, as the rate limiting step is the initial bimolecular reaction with O_2 and all subsequent processes are too rapid to affect these measured kinetics. Figure 1 (c) shows that the CID activation of *m/z* 127 results in a major signal at *m/z* 99 that is consistent with CO loss (28 Da) thus offering some support for the connection between these two ions. Isolation of *m/z* 127 with no additional CID activation, with trapping times extending for 5000 ms, produced no new signals (data not shown) leading us to conclude

that the production of m/z 99 is not the result of any ion activation imparted from trapping/isolation procedures nor it is from any gas-phase reaction process. In pyrolysis studies, neutral ortho-benzoquinone is known to lose CO to form cyclopentadieneone.[42,43] Our previous study of gas-phase hydroxyphenyl + O_2 reactions showed that benzoquinone products are susceptible to prompt decarbonylation.[14] These details suggest that it is possible that prompt decarbonylation of UBQ (m/z 127) is the explanation for formation m/z 99.

There are some noteworthy differences in this present reaction compared to our previous hydroxyphenyl + O_2 studies. Here, the proportion of m/z 99 (the decarbonylation product) compared to the parent is significantly larger than in the ammonium-tagged benzoquinone where only traces of decarbonylation where detected.[14] In Scheme 3, reactions IIa and IIb are compared with corresponding heats of reaction (calculated using G3X-K) of -7.6 kcal mol^{-1} for the UBQ case and +2.1 kcal mol^{-1} for the ammonium-tagged benzoquinone. One complete decarbonylation pathway was calculated for UBQ and displayed in Figure 4, and shows a rate limiting barrier at 17 kcal mol^{-1} relative to the reactants. This barrier is significantly lower than the rate limiting barrier calculated for decarbonylation of both neutral benzoquinone (42 kcal mol^{-1}) and the ammonium-tagged benzoquinone (35 kcal mol^{-1}).[14] An issue, however, is that if the decomposition of UBQ is driven by excess internal energy from the oxidation reaction, then the 17 kcal mol^{-1} barrier on the UBQ decarbonylation pathway seems rather high, especially considering the formation of UBQ is a bi-molecular product pathway, calculated at -20.9 kcal mol^{-1} heat of reaction, where significant energy is expected to be imparted to the OH co-product; although granted it is a somewhat late barrier on that product pathway (with a 6.2 kcal mol^{-1} reverse barrier). Our conclusion is that it is likely there are another mechanistic pathway (or pathways) for this decarbonylation, perhaps ones that are more direct, that explain our result either on the peroxy radical surface or the UBQ surface. A direct three-body elimination channel from the peroxy radical surface would be -28.5 kcal/mol relative to the starting reactants as indicated in Figure 3.

Finally, with these calculations we are cautious about multi-reference issues particularly as many species contain three oxygen atoms in addition to the nitrogen lone-pair. T1 diagnostic values[44] values are calculated and are included in Figures 3 and 4 – some rate determining barriers have T1 values > 0.03 which indicate possible inadequacies with the single-reference treatment of those structures. So further computational treatments are required along with further insights into the carbonylation pathways of benzoquinone species.

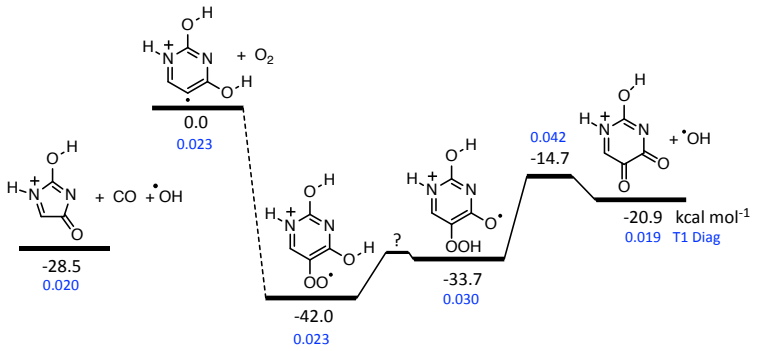

Figure 3: Potential energy scheme for the 5-dehydrouracilH$^+$ radical $+O_2$ calculated using the G3X-K method. Enthalpy values are provided relative to the entrance channel (black) in kcal mol^{-1} and T1 diagnostic values are presented in blue.

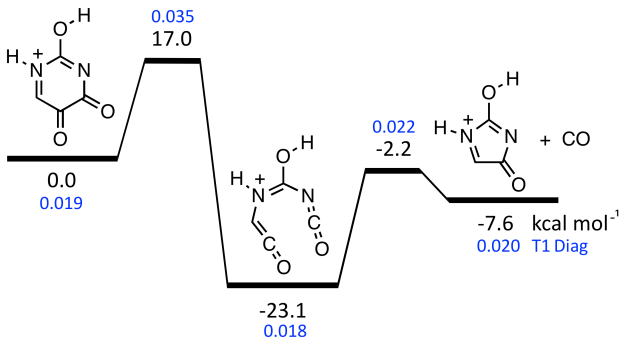

Figure 4: A decarbonylation pathway of the protonated 2-hydroxypyrimidine-4,5-dione ion calculated using the G3X-K method. Enthalpy values are provided relative to the entrance channel (black) in kcal mol^{-1} and T1 diagnostic values are presented in blue.

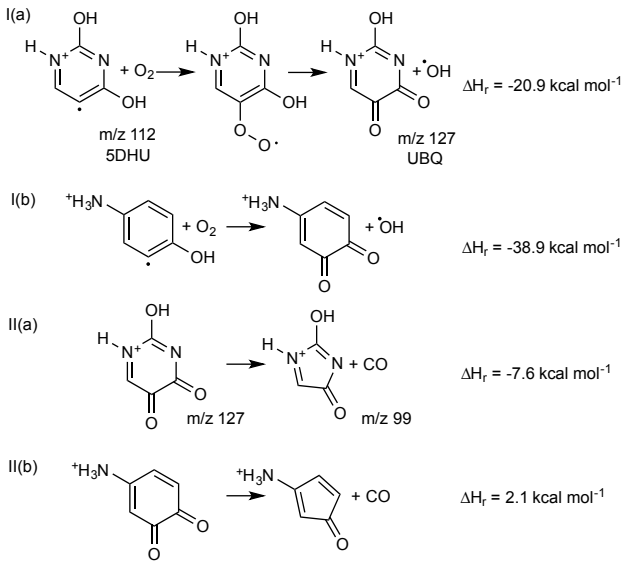

Scheme 3: Heat-of-reaction calculations comparing similar pathways for 5DHU and protonated aniline analogues

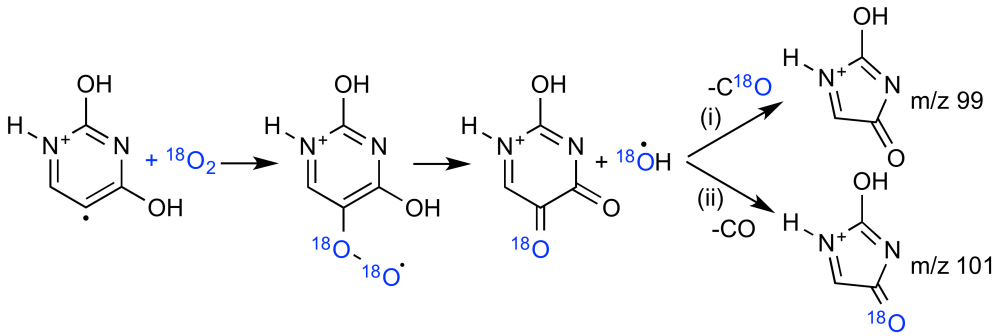

Scheme 4: Reaction pathways of 5DHU with $^{18}O_2$

Conclusion

In this study we have successfully utilised-gas phase photodissociation and ion-trap mass spectrometry to measure the second-order rate coefficient of the 5-dehydrouracilH^+ radical + O_2 reaction and determined the reaction efficiency. We have undertaken the first direct product studies of this reaction and analysed product structures. The 5-dehydrouracilH^+ distonic radical cation undergoes oxygen addition to form a peroxyl radical intermediate before losing an OH radical to form protonated 2-hydroxypyrimidine-4,5-dione (UBQ). A lower m/z product ion is also detected, which is consistent with a UBQ decarbonylation reaction that is assigned as 5-membered cyclic ketone species. But questions still remain around the formation of this product whether it is the result of a three-body elimination channel from the peroxy radical surface or if its a sequential process of decarbonylation following the formation of UBQ.

The formation of the protonated 5DHU radical cation within a biological system under aerobic conditions could initiate the formation of a quinone species and concomitant OH radical generation. It also evident that observation of an OH elimination channel in gas-phase studies is a general characteristic reaction O_2 reactions with phenyl radicals with and an *ortho* –OH group.

Supporting Information

A table of calculated relative energies for isomers of 5-dehydrouracilH^+ radical. CID mass spectrum of protonated 5-iodouracil. Product mass spectrum following CID of protonated 5-iodouracil and subsequent isolation and storage of m/z 112 in the presence of O_2.

Acknowledgement

The authors are grateful for the financial support of the Australian Research Council through the Discovery programs AJT: DP130100862, SJB: DP140101237 and AJT & SJB: DP170101596. The authors also acknowledge the generous allocation of computing resources by the NCI National Facility (Canberra, Australia) under the Merit Allocation Scheme. JPB and MBP each acknowledge support from an Australian Postgraduate Awards.

References

(1) Chen, T.; Cook, G. P.; Koppisch, A. T.; Greenberg, M. M. Investigation of the Origin of the Sequence Selectivity for the 5-Halo-2-deoxyuridine Sensitization of DNA to Damage by UV-Irradiation. *J. Am. Chem. Soc.* **2000**, *122*, 3861–3866.

(2) Willis, M. C.; Hicke, B. J.; Uhlenbeck, O. C.; Cech, T. R.; Koch, T. H. Photocrosslinking of 5-Iodouracil-Substituted RNA and DNA to Proteins. *Science* **1993**, *262*, 1255–1257.

(3) Xu, Y.; Sugiyama, H. Photochemical Approach to Probing Different DNA Structures. *Angew. Chem Int. Ed.* **2006**, *45*, 1354–1362.

(4) Rak, J.; Chomicz, L.; Wiczk, J.; Westphal, K.; Zdrowowicz, M.; Wityk, P.; Żyndul, M.; Makurat, S.; Golon, Ł. Mechanisms of Damage to DNA Labeled with Electrophilic Nucleobases Induced by Ionizing or UV Radiation. *J. Phys. Chem. B.* **2015**, *119*, 8227–8238.

(5) Tashiro, R.; Nakamura, K.; Sugiyama, H. Photoreaction of Iodouracil in DNA Duplex; C–I Bond is Cleaved via Two Different Pathways 'Homolysis and Heterolysis'. *Tetrahedron Lett.* **2008**, *49*, 428431.

(6) Wang, C.-R.; Lu, Q.-B. Molecular Mechanism of the DNA Sequence Selectivity of

5-Halo-2-Deoxyuridines as Potential Radiosensitizers. *J. Am. Chem. Soc.* **2010**, *132*, 14710–14713.

(7) Dai, X.; Song, D.; Liu, K.; Su, H. Photoinduced C-I Bond Homolysis of 5-Iodouracil: A Single Predissociation Pathways. *J. Chem. Phys.* **2017**, *146*, 025103.

(8) Kossoski, F.; do N. Varella, M. T. Negative Ion States of 5-Bromouracil and 5-Iodouracil. *Phys. Chem. Chem. Phys.* **2015**, *17*, 17271–17278.

(9) Wiczk, J.; Miloch, J.; Rak, J. UV Induced Strand Breaks in Double-Stranded DNA Labeled with 5–Bromouracil: Frank or Secondary. *J. Phys. Chem. Lett.* **2013**, *4*, 4014–4018.

(10) Schyman, P.; bo Zhang, R.; Eriksson, L. A.; Laaksonen, A. Hydrogen Abstraction from Deoxyribose by a Neighbouring Uracil-5-yl Radical. *Phys. Chem. Chem. Phys.* **2007**, *9*, 5975–5979.

(11) Cook, G. P.; Chen, T.; Koppisch, A. T.; Greenberg, M. M. The Effects of Secondary Structure and O_2 on the Formation of Direct Strand Breaks upon UV Irradiation of 5-Bromodeoxy-Uridine Containing Oligonucleotides. *Chemistry & Biology* **1999**, *6*, 451–459.

(12) Doddridge, Z. A.; Warner, J. L.; Cullis, P. M.; Jones, G. D. D. UV-Induced Strand Break Damage in Single Stranded Bromodeoxyuridine-Containing DNA Oligonucleotides. *Chem. Commun.* **1998**, 1997–1998.

(13) Schyman, P.; Eriksson, L. A.; Laaksonen, A. Hydrogen Abstraction from Deoxyribose by a Neighboring 3'-Uracil Peroxyl Radical. *J. Phys. Chem. B.* **2009**, *113*, 6574–6578.

(14) Prendergast, M. B.; Kirk, B. B.; Savee, J. D.; Osborn, D. L.; Taatjes, C. A.; Masters, K.-S.; Blanksby, S. J.; Silva, G.; Trevitt, A. J. Formation and Stability of Gas-Phase

o-Benzoquinone from Oxidation of ortho-Hydroxyphenyl: a Combined Neutral and Distonic Radical Study. *Phys. Chem. Chem. Phys.* **2016**, *18*, 4320–4332.

(15) Salpin, J.-Y.; Haldys, V.; Steinmetz, V.; Léon, E.; Yáñez, M.; Montero-Campillo, M. Protonation of methyluracils in the gas phase: The particular case of 3-methyluracil. *Int. J. Mass Spec.* **2017**, DOI:10.1016/j.ijms.2017.05.004.

(16) Wu, R.; Yang, B.; Frieler, C.; Berden, G.; Oomens, J.; Rodgers, M. Diverse Mixtures of 2,4-Dihydroxy Tautomers and O4 Protonated Conformers of Uridine and 2'-Deoxyuridine Coexist in the Gas Phase. *Phys. Chem. Chem. Phys.* **2015**, *17*, 25978–25988.

(17) Wu, R.; Rodgers, M. Tautomerization Lowers the Activation Barriers for N–Glycosidic Bond Cleavage of Protonated Uridine and 2'–Deoxyuridine. *Phys. Chem. Chem. Phys.* **2016**, *18*, 24451–24459.

(18) Williams, P. E.; Jankiewicz, B. J.; Yang, L.; Kenttämaa, H. I. Properties and Reactivity of Gaseous Distonic Radical Ions with Aryl Radical Sites. *Chem. Rev.* **2013**, *113*, 6949–6985.

(19) Kirk, B. B.; Harman, D. G.; Kenttämaa, H. I.; Trevitt, A. J.; Blanksby, S. J. Isolation and Characterization of Charge-Tagged Phenylperoxyl Radicals in the Gas Phase: Direct Evidence for Products and Pathways in Low Temperature Benzene Oxidation. *Phys. Chem. Chem. Phys.* **2012**, *14*, 16719–16730.

(20) Widjaja, F.; Jin, Z.; Nash, J. J.; Kenttämaa, H. I. Direct Comparison of Solution and Gas-Phase Reactions of the Three Distonic Isomers of the Pyridine Radical Cation with Methanol. *J. Am. Chem. Soc.* **2012**, *134*, 2085–2093.

(21) Donald, W. A.; Khairallah, G. N.; O'Hair, R. A. J. The Effective Temperature of Ions Stored in a Linear Quadrupole Ion Trap Mass Spectrometer. *J. Am. Soc. Mass Spectrom.* **2013**, *24*, 811–815.

(22) Harman, D. G.; Blanksby, S. J. Investigation of the Gas Phase Reactivity of the 1-Adamantyl Radical Using a Distonic Radical Anion Approach. *Org. Biomol. Chem.* **2007**, *5*, 3495–3503.

(23) Ly, T.; Julian, R. R. Residue-Specific Radical-Directed Dissociation of Whole Proteins in the Gas Phase. *J. Am. Chem. Soc.* **2008**, *130*, 351–385.

(24) Frisch, M. J.; Trucks, G. W.; Schlegel, H. B.; Scuseria, G. E.; Robb, M. A.; Cheeseman, J. R.; Scalmani, G.; Barone, V.; Mennucci, B.; Petersson, G. A. *et al*, Gaussian 09. 2009.

(25) Chan, B.; Deng, J.; Radom, L. G4(MP2)-6X: A Cost-Effective Improvement to G4(MP2). *J. Chem. Theory Comput.* **2011**, *7*, 112120.

(26) da Silva, G. G3X-K theory: A Composite Theoretical Method for Thermochemical Kinetics. *Chem. Phys. Lett* **2013**, *558*, 109–113.

(27) Nelson, C.; McCloskey, J. Collision-Induced Dissociation of Uracil and its Derivatives. *J. Am. Soc. Mass Spectrom.* **1994**, *5*, 339–349.

(28) Beach, D.; Gabryelski, W. Revisiting the Reactivity of Uracil During Collision Induced Dissociation: Tautomerism and Charge-directed Processes. *J. Am. Soc. Mass Spectrom.* **2012**, *23*, 858–868.

(29) Sadr-Arani, L.; Mignon, P.; Chermette, H.; Douki, T. Theoretical and Experimental Study of the Fragmentation of Protonated Uracil. *Chem. Phys. Lett.* **2014**, *605-606*, 108114.

(30) Molina, E. R.; Ortiz, D.; Salpin, J.-Y.; Spezia, R. Elucidating Collision Induced Dissociation Products and Reaction Mechanisms of Protonated Uracil by Coupling Chemical Dynamics Simulations with Tandem Mass Spectrometry Experiments. *J. Mass Spectrom.* **2015**, *50*, 1340–1351.

(31) Thoen, K. K.; Pérez, J.; Ferra, J. J.; Kenttämaa, H. I. Synthesis of Charged Phenyl Radicals and Biradicals by Laser Photolysis in a Fourier-Transform Ion Cyclotron Resonance Mass Spectrometer. *J. Am. Soc. Mass Spectrom.* **1998**, *9*, 1135–1140.

(32) Bakker, J.; Sinha, R.; Besson, T.; Brugnara, M.; Tosi, P.; Salpin, J.-Y.; Maître, P. Tautomerism of Uracil Probed via Infrared Spectroscopy of Singly Hydrated Protonated Uracil. *J. Phys. Chem. A* **2008**, *112*, 12393–12400.

(33) Berdakin, M.; Féraud, G.; Dedonder-Lardeux, C.; Jouvet, C.; Pino, G. Excited States of Protonated DNA/RNA Bases. *Phys. Chem. Chem. Phys.* **2014**, *16*, 10643–10650.

(34) Salpin, J.-Y.; Guillaumont, S.; Tortajada, J.; MacAleese, L.; Lemaire, J.; Maitre, P. Infrared Spectra of Protonated Uracil, Thymine and Cytosine. *Chem. Phys. Chem.* **2007**, *8*, 2235–2244.

(35) Pedersen, S. Ø.; Byskov, C. S.; Turecek, F.; Nielsen, S. B. Structures of Protonated Thymine and Uracil and Their Monohydrated Gas-Phase Ions from Ultraviolet Action Spectroscopy and Theory. *J. Phys. Chem. A* **2014**, *118*, 4256–4265.

(36) Féraud, G.; Esteves-López, N.; Dedonder-Lardeux, C.; Jouvet, C. UV Spectroscopy of Cold Ions as a Probe of the Protonation Site. *Phys. Chem. Chem. Phys.* **2015**, *17*, 25755–25760.

(37) Eichelberger, B. R.; Snow, T. P.; Bierbaum, V. M. Collision Rate Constants for Polarizable Ions. *J. Am. Soc. Mass Spectrom.* **2003**, *14*, 501–505.

(38) Prendergast, M. B.; Cooper, P. A.; Kirk, B. B.; da Silva, G.; Blanksby, S. J.; Trevitt, A. J. Hydroxyl Radical Formation in the Gas Phase Oxidation of Distonic 2–Methylphenyl Radical Cations. *Phys. Chem. Chem. Phys.* **2013**, *15*, 20577–20584.

(39) Moore, B. N.; Blanksby, S. J.; Julian, R. R. Ion–molecule Reactions Reveal Facile Radical Migration in Peptides. *Chem. Commun.* **2009**, *0*, 5015–5017.

(40) da Silva, G.; Chen, C. C.; Bozzelli, J. W. Toluene Combustion: Reaction Paths, Thermochemical Properties, and Kinetic Analysis for the Methylphenyl Radical + O_2 Reaction. *J. Phys. Chem. A* **2007**, *111*, 8663–8676.

(41) Ray, D. J. M.; Redfern, A.; Waddington, D. J. Gas-Phase Oxidation of Alkenes: Decomposition of Hydroxy-Substituted Peroxyl Radicals. *J. Chem. Soc., Perkin Trans. 2* **1973**, 540–543.

(42) Scheer, A. M.; Mukarakate, C.; Robichaud, D. J.; Nimlos, M. R.; Ellison, G. B. Thermal Decomposition Mechanisms of the Methoxyphenols: Formation of Phenol, Cyclopentadienone, Vinylacetylene, and Acetylene. *J. Phys. Chem. A*. **2011**, *115*, 13381–13389.

(43) Robichaud, D. J.; Scheer, A. M.; Mukarakate, C.; Ormond, T. K.; Buckingham, G. T.; Ellison, G. B.; Nimlos, M. R. Unimolecular Thermal Decomposition of Dimethoxybenzenes. *J. Chem. Phys.* **2014**, *140*, 234302.

(44) Lee, T. J.; Taylor, P. R. A Diagnostic for Determining the Quality of Single-Reference Electron Correlation Methods. *Int. J. Quantum Chem.* **1989**, *36*, 199–207.

TOC Graphic

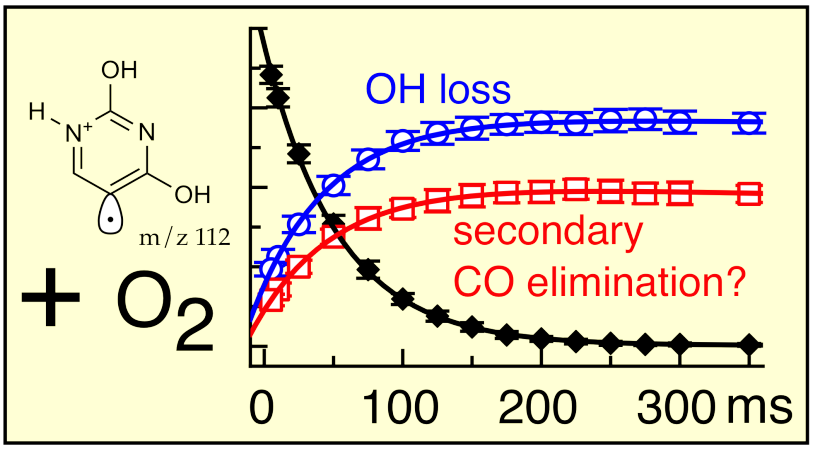
OH
H
N+
N
OH
m/z 112
+ O2
OH loss
secondary
CO elimination?
0
100
200
300 ms